



# New insights into anhydrobiosis using cellular dielectrophoresis-based characterization

Cite as: *Biomicrofluidics* **13**, 064113 (2019); doi: [10.1063/1.5126810](https://doi.org/10.1063/1.5126810)

Submitted: 5 September 2019 · Accepted: 4 November 2019 ·

Published Online: 15 November 2019



Mohamed Z. Rashed,<sup>1,a)</sup>  Clinton J. Belott,<sup>2,a)</sup> Brett R. Janis,<sup>2</sup> Michael A. Menze,<sup>2,b)</sup>  and Stuart J. Williams<sup>1,b)</sup>

## AFFILIATIONS

<sup>1</sup>Department of Mechanical Engineering, University of Louisville, 200 Sackett Hall, Louisville, Kentucky 40208, USA

<sup>2</sup>Department of Biology, University of Louisville, Life Sciences Building, Louisville, Kentucky 40292, USA

**Note:** This article is part of the special topic, Festschrift for Professor Hsueh-Chia Chang.

**a) Contributions:** M. Z. Rashed and C. J. Belott contributed equally to this work.

**b) Authors to whom correspondence should be addressed:** [michael.menze@louisville.edu](mailto:michael.menze@louisville.edu) and [stuart.williams@louisville.edu](mailto:stuart.williams@louisville.edu)

## ABSTRACT

Late embryogenesis abundant (LEA) proteins are found in desiccation-tolerant species from all domains of life. Despite several decades of investigation, the molecular mechanisms by which LEA proteins confer desiccation tolerance are still unclear. In this study, dielectrophoresis (DEP) was used to determine the electrical properties of *Drosophila melanogaster* (Kc167) cells ectopically expressing LEA proteins from the anhydrobiotic brine shrimp, *Artemia franciscana*. Dielectrophoresis-based characterization data demonstrate that the expression of two different LEA proteins, *Afr*LEA3m and *Afr*LEA6, increases cytoplasmic conductivity of Kc167 cells to a similar extent above control values. The impact on cytoplasmic conductivity was surprising, given that the concentration of cytoplasmic ions is much higher than the concentrations of ectopically expressed proteins. The DEP data also supported previously reported data suggesting that *Afr*LEA3m can interact directly with membranes during water stress. This hypothesis was strengthened using scanning electron microscopy, where cells expressing *Afr*LEA3m were found to retain more circular morphology during desiccation, while control cells exhibited a larger variety of shapes in the desiccated state. These data demonstrate that DEP can be a powerful tool to investigate the role of LEA proteins in desiccation tolerance and may allow to characterize protein-membrane interactions *in vivo*, when direct observations are challenging.

Published under license by AIP Publishing. <https://doi.org/10.1063/1.5126810>

## I. INTRODUCTION

Anhydrobiosis, or “life without water,” is a remarkable state of life where an organism has lost virtually all cellular water but is able to resume its life cycle upon rehydration. Understanding the molecular mechanism governing anhydrobiosis may lead to profound advances in engineering crop-desiccation tolerance and the ability to store biomedical relevant cell and tissue samples in the desiccated state as an alternative to cryopreservation. Anhydrobiosis-related intrinsically disordered (ARID) proteins are found in all known anhydrobiotic species, spanning all domains of life, and have been linked to the successful entry and exit from anhydrobiosis, but the molecular mechanisms underlying this phenomenon remain enigmatic.

The ability to enter and exit anhydrobiosis relies on an array of molecular mechanisms designed to repair and protect various cellular structures and macromolecules (e.g., DNA, RNA, proteins,

membranes, etc.). Common anhydrobiotic strategies observed in animals include the accumulation of protective osmolytes, particularly trehalose, as well as the expression of a variety of ARID proteins including late embryogenesis abundant (LEA) proteins<sup>1,2</sup> and tardigrade-specific intrinsically disordered proteins (TDPs). LEA proteins were originally discovered in plants and predominantly occur in the late embryogenesis stage of orthodox seeds but were later also found in other plant tissues and in anhydrobiotic animals.<sup>3</sup> Several sequence-based grouping methods for LEA proteins have been described, and this work will adapt the grouping scheme proposed by Tunnacliffe and Wise as a means to classify and organize groups of LEA proteins.<sup>4</sup>

This study focuses on two different LEA proteins from *A. franciscana*, *Afr*LEA3m and *Afr*LEA6, group 3 and 6 LEA proteins, respectively. While *Afr*LEA3m is a mitochondrial-targeted protein, it was shown to protect artificial membranes with a composition similar to the inner leaflet (i.e., inner side) of the plasma

membrane with the same efficacy as it protected artificial membranes with lipid composition mimicking the inner mitochondrial membrane.<sup>5–7</sup> Since the vast majority of mitochondrial proteins, including *Afr*LEA3m, are synthesized in the cytoplasm of the cell, it seems plausible that *Afr*LEA3m before its transport into the mitochondrial matrix could aid in protecting the plasma membrane during desiccation. While bioinformatic data suggest that *Afr*LEA3m can form amphipathic  $\alpha$ -helices during water stress to integrate into membranes, it remains experimentally undetermined if *Afr*LEA3m can directly or indirectly interact with membranes during water stress.<sup>8</sup> In contrast, *Afr*LEA6 localizes to the cytoplasm as judged by bioinformatics and confirmed by ectopic expression in Kc167 cells (data not shown).<sup>9</sup> While group 3 LEA proteins are commonly found in anhydrobiotic animals, *A. franciscana* is the only known anhydrobiotic animal to express a group 6 LEA protein, making it an interesting target for further study. Furthermore, bioinformatics does not suggest that *Afr*LEA6 can fold into amphipathic  $\alpha$ -helices during water stress, making it a good candidate for comparison to *Afr*LEA3m.

AC-electrokinetic based techniques such as dielectrophoresis,<sup>10–15</sup> electrorotation (eROT),<sup>16–19</sup> and electrochemical impedance spectroscopy (EIS)<sup>20–23</sup> have been used to investigate and analyze the properties of biological systems. DEP measures electrical properties by applying a nonuniform electric field to a liquid media of a known conductivity containing suspension of cells.<sup>24–27</sup> The non-uniform electrical field will induce a dipole within each cell; the induced translation of each cell in the electrical field depends on their phenotype, i.e., permittivity and conductance properties of the membrane and the cytoplasm as well as the conductivity of the solution. In this study, dielectrophoresis was used to gain insights into the molecular mechanisms of cellular protection during water stress conferred by *Afr*LEA3m and *Afr*LEA6, two LEA proteins from the anhydrobiotic brine shrimp, *Artemia franciscana*. Extracted DEP-based characterization data in this study demonstrate that the expression of LEA proteins from *A. franciscana* in desiccation sensitive cells from the fruit fly *D. melanogaster* has a pronounced impact on cytoplasmic conductivity and membrane capacitance. These results show that DEP can offer a novel approach to gain insights into the molecular mechanisms of protections this elusive class of proteins offers during anhydrobiosis.

## II. METHODS

### A. Cells, culture, and transfections

Kc167 cells were purchased from the Drosophila Genomics Research Center (DGRC; Bloomington, IN). Cells were cultured on 100 or 60 mm cell culture-treated dishes (Corning Incorporated, Corning NY) in Schneider's media (Caisson, USA) supplemented with 10% heat-inactivated fetal bovine serum (FBS) (Atlanta Biologicals, Lawrenceville, GA). Transfections were performed as previously described with the exception that Schneider's media was used in place of M3+BPYE medium and that 2.0 mg/ml G418 (ultrapure; VWR International) was used to select transfected cells and to generate and maintain stable cell lines.<sup>7</sup> The *pAc5-STABLE2-neo* vector was acquired from Addgene (Cambridge, MA). For additional information on the *pAc5-STABLE2-neo* vector, please see the Results and Discussions and Ref. 28. Immunoblotting with primary

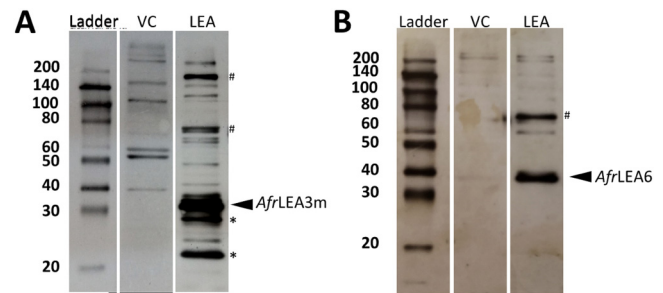


**FIG. 1.** Immunoblots confirming expression of (a) *Afr*LEA3m (~31 kDa<sup>5</sup>) in Kc167 cells. Several possible higher-order structures were also identified (#) as well as breakdown products (\*). Blotting results for vector control cells (VC) stably transfected with the expression vector but lacking inserted LEA proteins are shown for comparison. (b) *Afr*LEA6 expression in Kc167 cells. The apparent Mw was about 8 kDa larger than expected (~27 kDa<sup>9</sup>). The increased apparent Mw might be related to post-translational modification and the known behavior of some LEA proteins to migrate slower during SDS-PAGE than most non-LEA proteins. One higher-order structure was also identified (#).

antibodies (Aves Labs Inc., Tigard, OR) raised against *Afr*LEA6 or *Afr*LEA3m was performed on all cell lines to confirm transgenic protein expression<sup>9,29</sup> (Fig. 1).

SDS-PAGE and Western blot analyses were performed as previously described.<sup>7</sup> However, primary polyclonal antibodies raised against purified *Afr*LEA6 and *Afr*LEA3m (Aves Labs Inc., Tigard, OR; 1:5000 dilution) and HRP-linked goat antihen secondary antibodies (Aves Labs Inc., Tigard, OR; 1:5000 dilution) were used for detection.

### B. SEM imaging

Kc167 cells were plated onto an aluminum SEM stage at a concentration of  $2 \times 10^6$  cells/ml. The cells were allowed to attach to the stage for 1 h in a humidified chamber at 25 °C. Culture media was removed, and cells were then dried overnight at 10% relative humidity. The dried samples were sputter coated with an 18 nm film of gold and palladium and examined using a Zeiss Supra 35 VP scanning electron microscope with an electron high tension voltage of 15–20 kV.

### C. Dielectrophoresis

To collect cells and remove cell-culture medium, Kc167 cells were centrifuged at 400 g for 2 min at room temperature. The cellular pellets were resuspended in 10 ml of medium consisting of 85 g/l sucrose plus 3 g/l glucose, 11 mg/l CaCl<sub>2</sub>, and 24 mg/l MgCl<sub>2</sub>, ~360 mOsmol/kg. In experiments using hypertonic media, the osmolarity was brought to ~560 and ~760 mOsmol/kg with an additional 200 and 400 mM sucrose, respectively. To ensure complete removal of cell-culture medium, Kc167 cells were pelleted again and the final resuspension volume was approximately 1 ml. The final conductivity of the medium was adjusted to 5 mS/m using phosphate buffered saline (PBS) and the desired conductivity was verified with a conductivity meter (HORIBA Ltd., Koyoto, Japan). The number of cells was enumerated using a hemocytometer and adjusted to

approximately  $5\text{--}8 \times 10^6$  cells/ml ( $\pm 10\%$ ) for the DEP measurement. In general, one sample of 5 ml of cells,  $n_{bio}$ , in suspension can provide, on average, approximately 10–12 technical repeats,  $n_{tec}$ , of data sets with a total number of trials,  $n = n_{bio} \times n_{tec}$ . The 3DEP (Deptech, Ringmer, UK) platform was used to study the electrical properties of the cell. The experimental setup and electrode arrangement were used as described by Labeed *et al.*<sup>30</sup> To operate the instrument, cells are injected inside a microchip containing 20 microwells (3DEP 806), consisting of layers of embedded electrodes. Next, the chip is mounted on a camera setup where a light beam is directed from the top of the chip. An AC signal of 10  $V_{pp}$  and frequencies between 3 kHz and 40 MHz (at 5 frequencies per decade) are applied to all microwells simultaneously and the intensity of light passing through the microwells is then recorded concurrently. The intensity of light changes depending on the movement of the cells by the DEP force,  $F_{DEP}$ , exerted on them is

$$F_{DEP} = 2\pi\epsilon_s r^3 \Re[F_{cm}(\omega)] \nabla E^2. \quad (1)$$

$F_{DEP}$  is the force exerted on a particle of radius  $r$  in a medium of permittivity  $\epsilon_s$  within an electric field,  $E$ . The dielectric properties of the cell govern its movement within the nonuniform electric field. A single shell model was used which approximates cells as spheres of the cytoplasm of conductivity,  $\sigma_c$ , and permittivity,  $\epsilon_c$ , surrounded by a membrane of conductivity,  $\sigma_{mem}$ , and permittivity,  $\epsilon_{mem}$ , suspended in a medium of conductivity,  $\sigma_s$ , and permittivity,  $\epsilon_s$ . This simplified model offers a solvable number of parameters for a DEP spectrum, which is related to the data output of the 3DEP platform. This is represented by the Clausius-Mossotti factor,  $F_{cm}(\omega)$ , which is a function of frequency, conductance, and permittivities of cell cytoplasm, membrane, and suspending media, thus

$$F_{cm}(\omega) = \left( \frac{\epsilon_{cell}^* - \epsilon_s^*}{\epsilon_{cell}^* + 2\epsilon_s^*} \right), \quad (2)$$

$$\epsilon_{cell}^* = \epsilon_s^* \frac{\left( \frac{r}{r-d} \right)^2 + 2 \frac{\epsilon_c^* - \epsilon_{mem}^*}{\epsilon_c^* + 2\epsilon_{mem}^*}}{\left( \frac{r}{r-d} \right)^3 - \frac{\epsilon_c^* - \epsilon_{mem}^*}{\epsilon_c^* + 2\epsilon_{mem}^*}}, \quad (3)$$

where  $\epsilon_{cell}^*$  is the effective complex permittivity of the cell, with  $r$  and  $d$  being the radius of the cell and membrane thickness ( $d=10$  nm), respectively.  $\epsilon^* = \epsilon - j\sigma/\omega$  represents the complex permittivity and is a function of the permittivity  $\epsilon$ , conductivity  $\sigma$ , and angular frequency of the electric field  $\omega$ . Hence, based on the sign of  $\Re[F_{cm}(\omega)]$ , cells will experience either a negative dielectrophoresis (nDEP) or a positive (pDEP) force. Cells experiencing an nDEP force will be centered in the middle of the microwell where they will be blocking the light (i.e., repelled to field minima). Conversely, the cells experiencing a pDEP force will be attracted toward the perimeter of the microwell, and more light will pass through the center of the microwells (i.e., attracted to field maxima).

Light intensity, in each microwell, was measured for 30 s sweeping a frequency range from 3 kHz to 40 MHz. The light intensity vs frequency spectrum generated was next fitted by an iterative least

square method<sup>30</sup> to Eqs. (1)–(3) to yield individual values of membrane and cytoplasmic conductivity as well as specific membrane capacitance,  $c = \epsilon_{mem}/d$ . 3DEP light intensity bands from 4 to 9, from the platform spectrum output, were only selected for each experiment to be fitted, resulting in a better DEP spectrum fitting correlation coefficient  $R > 0.97$  (Fig. 2). Cells were measured immediately ( $<17$  min) after being suspended into the DEP media to

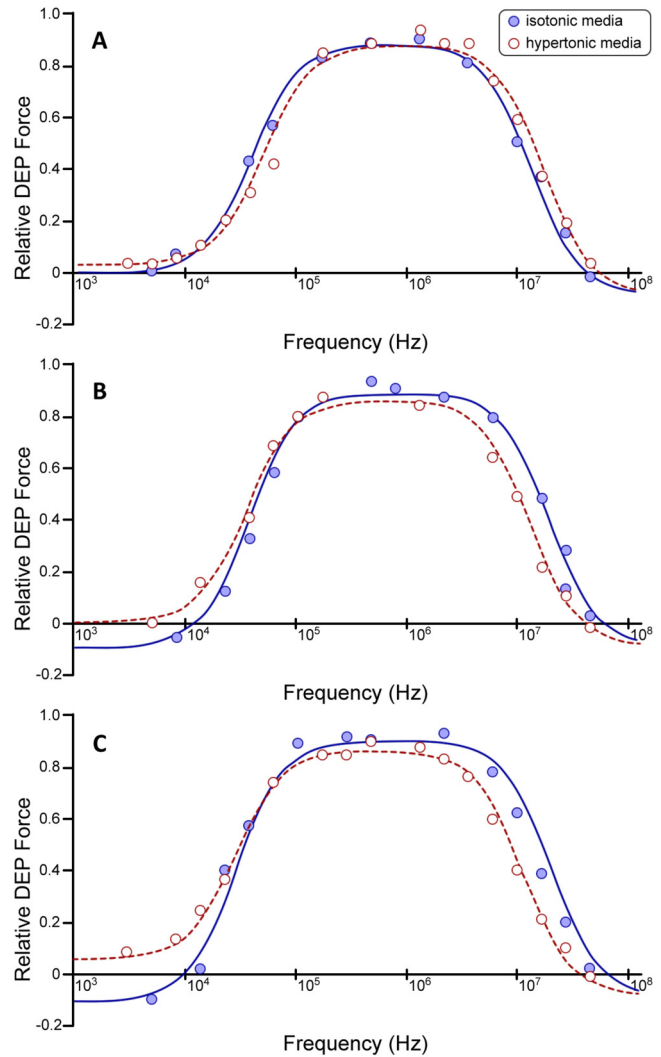


**FIG. 2.** Dielectrophoretic properties of Kc167 cells. Comparison of DEP spectra produced from suspending cells in isotonic media ( $\sim 360$  mOsmol/kg; blue) and hypertonic media ( $\sim 760$  mOsmol/kg; red) for (a) Kc167 vector control (VC) cells averaged DEP spectra ( $n = 68$  and  $n = 61$ ). (b) Kc167 cells expressing the AfrLEA3m protein averaged DEP spectra ( $n = 72$  and  $n = 58$ ). (c) Kc167 cells expressing the AfrLEA6 protein averaged DEP spectra ( $n = 72$  and  $n = 57$ ). The solid line curves are fits of Eqs. (1)–(3), see Sec. II. The y-axis relative polarizability is a function of the  $[F_{cm}(\omega)]$  factor with positive values equivalent to pDEP and negative values equivalent to nDEP. The respective correlation coefficient,  $R$ , values for all fitted curves were  $R > 0.97$ .

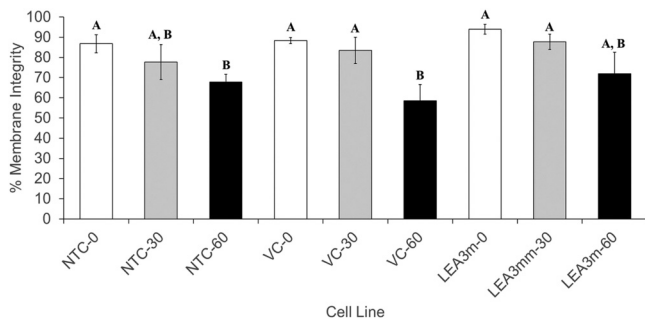


**FIG. 3.** Viability of nontransfected controls (NTC), vector controls (VC), and *Afr*LEA3m expressing (LEA3m) of Kc167 cells is significantly reduced when incubated for up to 60 min in low ionic strength (<6.5 S/m) isotonic sucrose medium (~360 mOsmol/kg). White bars represent 0 min incubation, gray bars represent 30 min incubation, and black bars represent 60 min incubation. Letters denote significance (i.e., “A” and “B” are significantly different from one another, but neither are significantly different from “A, B”) ( $\pm$  SD;  $P < 0.05$ ; one-way ANOVA).

minimize artifacts due to cell stress by the nonphysiological ion composition of the medium. The time to collect and characterize approximately 10–13 samples using the 3DEP platform takes only 15–17 min. To investigate the effect of the DEP buffer on cell viability and potentially changes in the measured parameters, we studied Kc167 cells’ viability in isotonic and hyperosmotic DEP media for up to 1 h. No significant changes in cell viability were found for up to 30 min and all

other experiments were completed in under 20 min ( $\pm$  SD;  $P > 0.05$ ; one-way ANOVA, Fig. 3). Furthermore, no significant changes in the resultant DEP spectrum of Kc167 cells characterized within 30 min was observed ( $\pm$  SD;  $P > 0.05$ ; one-way ANOVA, Fig. 3).

**III. RESULTS AND DISCUSSIONS**

In this study, a detailed characterization of the electrical properties of Kc167 cells from *D. melanogaster* and the changes that occur in these properties in response to acute osmotic stresses have been achieved. Using ectopic protein-expression models, modulations in the osmotic-stress response could be correlated to molecular mechanisms of cellular protection conferred by two LEA proteins that ameliorate water-stress damage in the anhydrobiotic embryos of *A. franciscana*.<sup>31</sup> Previous studies conducted with artificial liposomes have indicated that *Afr*LEA3m can directly interact with phospholipid bilayers during severe water stress.<sup>5</sup> Based on these data, it was hypothesized that the specific membrane capacitance of Kc167 cells expressing *Afr*LEA3m will increase during water stress and that the specific membrane conductance be unaltered if *Afr*LEA3m was indeed interacting directly with the plasma membrane during moderate osmotic stress (~760 mOsmol/kg). To test this hypothesis, a dielectrophoresis-based platform was used to characterize the cytoplasmic conductivity, the specific membrane capacitance, and the specific membrane conductance of cells in isotonic sucrose medium (~360 mOsmol/kg) with a low ionic strength (<6.5 S/m), and hypertonic media of either 560 or 760 mOsmol/kg adjusted by addition of sucrose to reach the

**TABLE I.** Extracted cellular electrical constants (cytoplasm conductivity, S/m; specific membrane capacitance, mF/m<sup>2</sup>; and conductance, S/m<sup>2</sup>) of Kc167 cells.

	Isotonic sucrose/glucose medium + CaCl <sub>2</sub> and MgCl <sub>2</sub> (360 mOsmol/kg)	Hypertonic sucrose/glucose medium (+200 mM sucrose) (560 mOsmol/kg)	Hypertonic sucrose/glucose medium (+400 mM sucrose) (760 mOsmol/kg)
<i>Cytoplasm conductivity (S/m)</i>			
Kc167 vector control (VC)	0.152 ± 0.016 (n = 68)	0.192 ± 0.009 <sup>a</sup> (n = 62)	0.189 ± 0.012 <sup>a</sup> (n = 61)
Nontransfected control	0.162 ± 0.014 (n = 18)		
VC-dead	0.032 ± 0.002 <sup>b</sup> (n = 7)		
<i>Afr</i> LEA3m	0.215 ± 0.018 <sup>b</sup> (n = 72)	0.172 ± 0.007 <sup>a,b</sup> (n = 63)	0.139 ± 0.014 <sup>a,b</sup> (n = 58)
<i>Afr</i> LEA6	0.23 ± 0.0186 <sup>b</sup> (n = 72)	0.188 ± 0.0163 <sup>a</sup> (n = 61)	0.126 ± 0.015 <sup>a,b</sup> (n = 57)
<i>Specific membrane capacitance (mF/m<sup>2</sup>)</i>			
Kc167 vector control (VC)	10 ± 1.6 (n = 68)	11.4 ± 1.18 (n = 62)	12.6 ± 1.3 (n = 61)
Nontransfected control	10.5 ± 1.6 (n = 18)		
VC-dead	2.7 ± 0.06 <sup>b</sup> (n = 7)		
<i>Afr</i> LEA3m	9.8 ± 1.2 (n = 72)	14.7 ± 1.6 <sup>a,b</sup> (n = 63)	14.2 ± 0.8 <sup>a,b</sup> (n = 58)
<i>Afr</i> LEA6	11.8 ± 1.8 (n = 72)	12.4 ± 1.53 (n = 61)	15.0 ± 3.0 (n = 57)
<i>Specific membrane conductance (S/m<sup>2</sup>)</i>			
Kc167 vector control (VC)	793 ± 63 (n = 68)	1114 ± 80 <sup>a</sup> (n = 62)	1129 ± 132 <sup>a</sup> (n = 61)
Nontransfected control	812 ± 38 (n = 18)		
VC-Dead	503 ± 43 <sup>b</sup> (n = 7)		
<i>Afr</i> LEA3m	758 ± 75 (n = 72)	878 ± 73 <sup>b</sup> (n = 63)	915 ± 73 <sup>a,b</sup> (n = 58)
<i>Afr</i> LEA6	710 ± 42 (n = 72)	956 ± 62 <sup>a,b</sup> (n = 61)	1050 ± 110 <sup>a</sup> (n = 57)
<i>Cell diameter (μm)</i>	10 ± 0.23 (n = 7)	9.2 ± 0.31 (n = 10)	8.9 ± 0.21 (n = 10)

<sup>a</sup>Values differ significantly from the corresponding isotonic medium (one-way ANOVA;  $P < 0.05$ ), total number of trials,  $n = n_{bio}$  (~ 5–6) ×  $n_{tec}$ (~ 10–12).

<sup>b</sup>Values differ significantly from the corresponding control (one-way ANOVA;  $P < 0.05$ ), total number of trials,  $n = n_{bio}$  (~ 5–6) ×  $n_{tec}$ (~ 10–12).

desired osmolarity, to mimic water stress (Table I). The low ionic strength of the media was required to create a significant difference between media conductivity and that of the cytoplasm and membrane, thereby increasing the resolution of DEP measurements [Eq. (2)], hence, achieving better resolution. Conversely, relatively high media conductivity ( $\sim 100$  mS/m) will compromise the reliability of the DEP measurements by introducing other electrokinetic effects (e.g., Joule heating<sup>32</sup>). However, these DEP-compatible media may negatively impact cell viability over time, since the cells are deprived of several important components normally found in insect cell-culture media (e.g., monovalent ions, sugars, and amino acids). Not surprisingly, a significant decrease in the values of all three fitted parameters (cytoplasmic conductivity, the specific membrane capacitance, and the specific membrane conductance) was observed for control cells incubated in isotonic sucrose media for  $\sim 16$  h, where 100% of cells showed a collapse in membrane integrity (Table I, VC-Dead). Furthermore, the viability of cells in isotonic sucrose media was also significantly reduced after only 60 min of incubation for nontransfected control and vector control cells, indicating the time-sensitivity of the measurements (Fig. 3). However, there was no significant reduction in viability for up to 30 min of incubation for any cell line in all DEP media employed. Based on these data, all other measurements were completed within  $<18$  min to avoid artifacts caused by cell death. There was no significant difference observed in any fitted values between nontransfected control cells and vector control cells demonstrating that the expression of transgenic genes such as the aminoglycoside 3'-phosphotransferase to confer G418 resistance does not per se change the electrical properties of cells (Table I).

Interestingly, there was an  $\sim 41\%$  and  $\sim 51\%$  increase in the cytoplasmic conductivity of cells expressing *AfrLEA3m* and *AfrLEA6*, respectively, over vector controls under isotonic media conditions. The impact on cytoplasmic conductivity was surprising, given that the concentration of cytoplasmic ions is much higher than the concentrations of ectopically expressed proteins. Cytoplasmic conductivity is assumed to be primarily affected by the intracellular  $[K^+]$  and, to a lesser amount  $[Cl^-]$ , given their relatively high concentrations compared to other ions, charged molecules, and macromolecules. The specific membrane capacitance (i.e., the capacitance of the membrane normalized to the unit cell cross section and membrane area), is defined here as the ability of a membrane to hold an electric charge. By treating the membrane as a dielectric slab, with a relative permittivity ( $\epsilon_r$ ), that is flanked by two parallel plate electrodes that are distance ( $d$ ) apart, each with an area ( $A$ ), and a dielectric constant ( $\epsilon_0$ ), gives rise to the equation  $C_{mem} = (\epsilon_r)(\epsilon_0)/(d)$  (Farad per unit area). In reference to the cell, changes in the specific membrane capacitance can be affected by the dielectric constant,  $\epsilon_{mem}$  (determined by the composition of the membrane), the area of the membrane (i.e., morphology), and the thickness of the plasma membrane (particularly within the insulating hydrophobic tail region).<sup>33</sup> The specific membrane conductivity is simply the ability of an electric current to pass through the membrane and was generally thought to be primarily impacted by membrane thickness, gating state of ion channels, and area.<sup>34</sup> However, recent data have shown that an increase in ion efflux or influx can increase the specific membrane conductivity and concurrently decrease cytoplasmic conductivity, while both membrane thickness and area remain unchanged.<sup>35</sup> In the

absence of ion-channel involvement, any increase in membrane thickness should decrease both the membrane conductance and the capacitance, while an increase in the membrane area should increase both values.<sup>24</sup> It was hypothesized that *AfrLEA3m* would interact with the inner leaflet of the plasma membrane during acute osmotic stress. Bioinformatic analysis predicts that *AfrLEA3m* folds into amphipathic  $\alpha$ -helices during water stress, whereas *AfrLEA6* does not.<sup>8</sup> Amphipathic  $\alpha$ -helices are often associated with membrane interactions (i.e., a protein would be able to interact with charged phospholipid head groups, as well as their hydrophobic tail region). This may cause a change in its dielectric constant,  $\epsilon_{mem}$ , while not significantly impacting the membrane thickness and area (i.e., the specific membrane capacitance increases, while the specific membrane conductance would remain constant). In contrast, *AfrLEA6* was hypothesized to not interact with the inner leaflet of the plasma membrane, thereby any change (positive or negative) observed in the specific membrane conductance may lead to changes in the specific membrane capacitance.

Data in Table I show that the specific membrane conductance and capacitance were unaffected by the ectopic expression of either *AfrLEA3m* or *AfrLEA6*. The effect of both proteins on cytoplasmic conductivity could be mediated by direct or indirect interactions with ion channels causing an influx of monovalent ions (i.e., increasing the concentration of a simple electrolyte such as  $K^+$  or  $Na^+$  will theoretically increase the cytoplasmic conductivity). In the case of red blood cells, however, the specific membrane conductivity and cytoplasmic conductivity move in antiphase with rhythmic efflux of  $K^+$  ions.<sup>35</sup> The lack of  $K^+$  and  $Na^+$  in the employed DEP media and the presence of only minor amounts of divalent ions make a mechanism based on ion influx highly unlikely.

An alternative mechanism might be that, due to the highly hydrophilic and charged nature of *AfrLEA3m* and *AfrLEA6*, the mobility of monovalent ions surrounding *AfrLEA3m* and *AfrLEA6* is effectively higher than for VC cells, without actually changing ion concentration. This may increase the molar conductivity of the cytoplasm. Molar conductivity ( $\Lambda_m$ ) is defined as the relationship between electrolyte concentration ( $c$ ) and conductivity ( $\kappa$ ). In the equation  $\Lambda_m = (\kappa)/(c)$ , any increase in electrolyte concentration will decrease molar conductivity.<sup>33</sup> This is due to an increase in drag force being placed on a given diffusing ion as the concentration of ions of an opposite charge increases (i.e., Debye-Huckel theory). If the equation is written instead as  $\kappa = (\Lambda_m)(c)$ , then it becomes clear that an increase in molar conductivity at a constant ion concentration will increase cytoplasmic conductivity. This alternative mechanism is supported by molecular dynamics simulations of polyelectrolytes (highly charged polymers) and simple electrolytes, where increasing the concentration of polyelectrolytes increased the dispersion of ions around the polymers and thereby increased the molar conductivity of the ions.<sup>33</sup> In addition, the cytoplasmic conductivity of cells expressing *AfrLEA3m* or *AfrLEA6* progressively decreases as the cells were exposed to hypertonic solutions (Table I). This is in stark contrast to vector control cells, which displayed a cytoplasmic conductivity that progressively increased when exposed to increasingly hypertonic solutions. In the case where the electrolyte concentrations are increasing, as would be the case when osmotically active water is being pulled out of the cell due to hypertonic stress, conductivity should decrease if molar

conductivity decreases. However, the equation  $\kappa = (\Lambda_m)(c)$  does demonstrate that increasing ion concentrations in a cell should increase the conductivity of the cytoplasm. However, this assumes that the decrease in molar conductivity is sufficiently outweighed by the increase in electrolyte concentrations. This can be observed in vector control cells under osmotic stress, where a decrease in cell volume leads to a subsequent increase in intracellular ion concentrations and cytoplasmic conductivity. In the case of cells expressing *Afr*LEA3m and *Afr*LEA6, the observed decrease in cytoplasmic conductivity during hyperosmotic stress may be a result of a decrease in molar conductivity outweighing the increase in electrolyte concentration, leading to a net loss in cytoplasmic conductivity [i.e., in  $\kappa = (\Lambda_m)(c)$ , the decrease in  $(\Lambda)$  outweighs the increase in  $(c)$  and leads to a reduction in  $(\kappa)$ ]. These data suggest that, under isotonic conditions, LEA proteins are unentangled and increase the cytoplasmic conductivity by behaving as typical polyelectrolytes, thereby increasing cytoplasmic ion diffusivity.<sup>36</sup> During osmotic stress, the decrease in cellular volume may be sufficient to concentrate LEA proteins enough to shift their dynamics from a semidilute, unentangled regime to an entangled regime. Under entangled conditions, the effect of LEA proteins on ion diffusivity may be negated.<sup>36,37</sup>

When Kc167 cells were challenged with hyperosmotic stress (~570 and 760 mOsmol/kg), cells expressing *Afr*LEA3m experienced a sharp increase in specific membrane capacitance (~56%). However, specific membrane conductance did not significantly change when cells expressing *Afr*LEA3m were challenged with a moderate hypertonic stress of 570 mOsmol/kg. In the case of the osmotically stressed cells, the radius decreases by approximately (~11%) and, in turn, should increase the specific membrane capacitance by (~11%). However, this increase does not sufficiently explain the observed (~56%) increase in specific membrane capacitance. No apparent differences in cell morphology (aside from reported changes in cell diameter; Table I) were observed when cells were subjected to severe osmotic stress (~760 mOsmol/kg) and imaged with confocal microscopy (data not shown).

Further analysis of the data relies on two assumptions; first, the effective area of the membrane surface is changing, hence changing the capacitance of the membrane ( $C_{mem} = \phi \epsilon_0 \epsilon_r / d$ ), where  $\phi$  membrane topography parameter that represents the ratio of the actual membrane area of the cell to the membrane area ( $4\pi R^2$ ) that would form a perfectly smooth and spherical covering of the cytoplasm and it is proportional to the “roughness” of the membrane surface. Furthermore, cells subjected to the hypertonic media would shrink them causing the membrane to wrinkle leading to an increase in  $\phi$  ( $\approx 1.5$ ) and therefore  $C_m$ .<sup>24,38</sup> Similar results were observed for salivary gland cells (*Drosophila*, *Chironomids*, and *Sciarids*), where  $\phi$  ranged from 160 to 830.<sup>39</sup> Furthermore, the change in the membrane effective area is further proved by the data reporting a decrease in membrane capacitance of cells suspended in hypotonic media due to cell swelling and the opposite effect when suspended in hypertonic media.<sup>38,40–42</sup> However, it is also noted that this increase in  $C_{mem}$ , for Kc167 cells expressing either *Afr*LEA3m or *Afr*LEA6 suspended in 760 mOsmol/kg, does not mean the formation of blebs or shriveling of the membrane, as there was no indication of apoptosis or necrosis of the cells.<sup>43,44</sup> These data were supplemented with SEM imaging.

After complete desiccation for 18–24 h, cells expressing *Afr*LEA3m retained a more circular morphology than vector control cells, which displayed a variety of shapes and sizes [Figs. 4(a) and 4(b)]. In addition, cells expressing *Afr*LEA3m often displayed relatively large porelike structures that were never observed in vector control cells [Figs. 4(c) and 4(d)]. These porelike structures may be stress points where the membrane begun ripping apart but complete lysis was stopped due to the presence of *Afr*LEA3m. Indeed, vector control cells can often be seen with large tears that allows for the cytoplasm to leak out while desiccation is still occurring. Data in Table I show no significant difference in the membrane conductance of Kc167 cells expressing *Afr*LEA3m, indicating that the cell membrane is intact, and cells did not exhibit either necrosis or apoptosis. Moreover, this increase in the membrane conductance (~16%) for osmotically stressed *Afr*LEA3m can be attributed to the effective area of the membrane surface ( $G_{mem} = \phi G_0$ , where  $\phi \approx 1.2$ ) which is close to the actual increase in  $G_{mem}$  ( $\approx 1.5$ ). However, the increase in the membrane conductance of the Kc167 vector control could be attributed to the degradation of the plasma membrane.<sup>44</sup>

The second assumption states that the relative dielectric constant,  $\epsilon_r$ , and thickness,  $d$ , of the membrane are changing due to the expression of LEA proteins as well as osmotic stress imposed from the hypertonic media, with the relative dielectric constant,  $\epsilon_r$ , surprisingly increasing due to the expression of the LEA proteins. The presence of organelles, structures, or polypeptides such as LEA proteins will contribute to the internal dielectric properties of the cell. Several studies reported changes in the dielectric constant which in turn have an influence on the membrane capacitance.<sup>45–47</sup> Gentet *et al.*<sup>48</sup> showed a minor decrease in the membrane capacitance

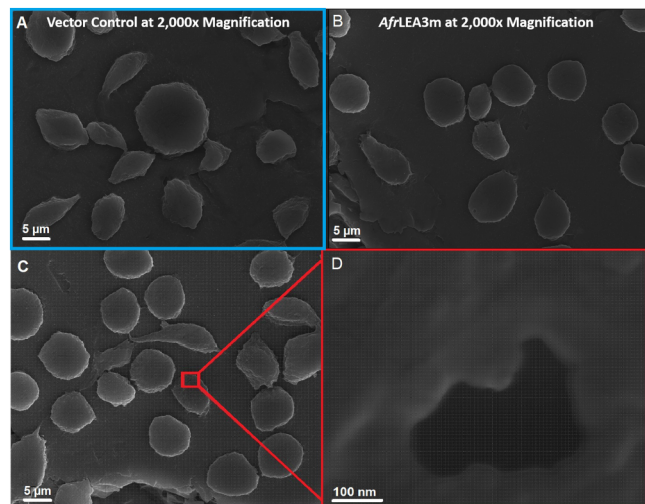


**FIG. 4.** SEM images demonstrating that cells expressing *Afr*LEA3m retain a more circular shape after complete desiccation and have porelike formations in their plasma membranes. Vector control (VC) cells (a) and cells expressing *Afr*LEA3m (b) and (c) were completely desiccated prior to imaging. (d) Pores were observed exclusively intact, desiccated *Afr*LEA3m cells. Scale bars for (a)–(c) represent 5  $\mu\text{m}$ , while the scale bar for (d) represents 100 nm.

(~6%) due to expressing glycine receptors and other membrane proteins in embryonic kidney cells (HEK-293). Similarly, Stoneman *et al.*<sup>49</sup> also reported a decrease in the membrane capacitance of yeast cells (~7%) overexpressing a G protein coupled receptor (Ste2p protein). In contrast to our work, these two experiments did not induce any osmotic stress on the cells being studied. The  $C_{mem}$  value mostly reflects the properties of the hydrophobic layer of the membrane, which is populated by the hydrocarbon tails of the phospholipids and hydrophobic segments of integral membrane proteins.<sup>50</sup> Considering that *Afr*LEA3m is expected to only fold into its native structure in response to water stress, the observed increase in the membrane capacitance under osmotic stress is not surprising. Therefore, Kc167 cells expressing *Afr*LEA3m will yield different membrane capacitance ( $C_{mem}$ ) and conductance ( $G_{mem}$ ) values when subjected to hyperosmotic stress. It should be noted that the porelike formations in the SEM images [Figs. 4(c) and 4(d)] only form in the completely dried state. In the case of porelike formations occurring during an osmotic stress of ~760 mOsmol/kg, the relative dielectric constant of the membrane would decrease by a factor of approximately one-fourth.<sup>24</sup> This is in contrast to the observed increase in the specific membrane capacitance in cells expressing *Afr*LEA3m. The formation of ~200–300 nm large pores would result in a loss of membrane integrity, but this was not observed during preparation of cells for hyperosmotic stress experiments (data not shown). Furthermore, our data suggest that *Afr*LEA3m is integrating, at least to some capacity, into the plasma membrane which agrees with previously published results that suggests *Afr*LEA3m protects membranes during water stress.<sup>5</sup>

Lacking any apparent propensity to form amphipathic  $\alpha$ -helices, *Afr*LEA6 is an ideal protein to compare to *Afr*LEA3m.<sup>8</sup> In comparison with *Afr*LEA3m, cells expressing *Afr*LEA6 experienced a significant increase in the membrane conductance, but not specific membrane capacitance, when challenged with moderate hyperosmotic stress (~570 mOsmol/kg). Furthermore, specific membrane capacitance for cells expressing *Afr*LEA6 was not significantly different from what was observed for vector control cells under all conditions. The observed increase in specific membrane conductance for cells expressing *Afr*LEA6, as well as vector control cells, is thought to be due to an efflux of monovalent ions (likely by gated ion channels) that is ameliorated when *Afr*LEA3m integrates into the membrane as well as the change in the effective area of the membrane surface (i.e.,  $\phi$ ) which influences both  $C_{mem}$  and  $G_{mem}$ .

#### IV. CONCLUSION

In summary, a dielectrophoresis-based platform was used to characterize the electrical properties of Kc167 cells from *D. melanogaster* expressing late embryogenesis abundant proteins from the anhydrobiotic embryos of *A. franciscana*. The increase in cytoplasmic conductivity observed in Kc167 vector control cells under osmotic stress is related to the reduction in cell volume and the increase in ion concentration. We hypothesize that the increase in cytoplasmic conductivity, for cells ectopically expressing *Afr*LEA3m or *Afr*LEA6, under isotonic conditions, is related to both LEA proteins behaving as typical polyelectrolytes increasing the diffusivity of cytoplasmic ions. Under osmotic-stress conditions, the protein dynamics may shift from an unentangled regime to a concentrated

regime which leads to a decrease in cytoplasmic conductivity. In the case of *Afr*LEA3m being activated during osmotic stress, then the increases in the specific membrane capacitance during hyperosmotic stress may be due to its direct interactions with the plasma membrane. The increase in specific membrane conductance observed in Kc167 vector control cells was related to changes in plasma membrane morphology during hyperosmotic stress. In contrast, for cells ectopically expressing LEA proteins, the increase in the specific membrane conductance is driven by a change in the effective area of their membrane surfaces in addition to any changes in membrane morphology that may occur during hyperosmotic stress. Altogether, these data support the utility of cellular DEP-based characterization as a powerful tool to identify protein-membrane interactions *in vivo* when direct observations are challenging.

#### ACKNOWLEDGMENTS

The authors would like to thank the National Science Foundation (NSF) for financially supporting this research under Grant No. IDBR-1550509 to S.J.W. and Grant No. IOS-1659970 to M.A.M.

#### REFERENCES

- <sup>1</sup>B. Janis, C. Belott, and M. A. Menze, "Role of intrinsic disorder in animal desiccation tolerance," *Proteomics* **18**, 1800067 (2018).
- <sup>2</sup>F. A. Hoekstra, E. A. Golovina, and J. Buitink, "Mechanisms of plant desiccation tolerance," *Trends Plant Sci.* **6**, 431–438 (2001).
- <sup>3</sup>S. C. Hand, M. A. Menze, M. Toner, L. Boswell, and D. Moore, "LEA proteins during water stress: Not just for plants anymore," *Annu. Rev. Physiol.* **73**, 115–134 (2011).
- <sup>4</sup>M. J. Wise and A. Tunnacliffe, "POPP the question: What do LEA proteins do?," *Trends Plant Sci.* **9**, 13–17 (2004).
- <sup>5</sup>D. S. Moore, R. Hansen, and S. C. Hand, "Liposomes with diverse compositions are protected during desiccation by LEA proteins from *Artemia franciscana* and trehalose," *Biochim. Biophys. Acta* **1858**, 104–115 (2016).
- <sup>6</sup>M. A. Menze, L. Boswell, M. Toner, and S. C. Hand, "Occurrence of mitochondria-targeted late embryogenesis abundant (LEA) gene in animals increases organelle resistance to water stress," *J. Biol. Chem.* **284**, 10714–10719 (2009).
- <sup>7</sup>M. R. Marunde, D. A. Samarajeewa, J. Anderson, S. Li, S. C. Hand, and M. A. Menze, "Improved tolerance to salt and water stress in *Drosophila melanogaster* cells conferred by late embryogenesis abundant protein," *J. Insect Physiol.* **59**, 377–386 (2013).
- <sup>8</sup>B. Janis, V. N. Uversky, and M. A. Menze, "Potential functions of LEA proteins from the brine shrimp *Artemia franciscana*—Anhydrobiosis meets bioinformatics," *J. Biomol. Struct. Dyn.* **36**, 3291–3309 (2018).
- <sup>9</sup>B. M. LeBlanc, M. T. Le, B. Janis, M. A. Menze, and S. C. Hand, "Structural properties and cellular expression of *Afr*LEA6, a group 6 late embryogenesis abundant protein from embryos of *Artemia franciscana*," *Cell Stress Chaperones* **24**(5), 979–990 (2019).
- <sup>10</sup>F. H. Labeed, H. M. Coley, and M. P. Hughes, "Differences in the biophysical properties of membrane and cytoplasm of apoptotic cells revealed using dielectrophoresis," *Biochim. Biophys. Acta* **1760**, 922–929 (2006).
- <sup>11</sup>L. M. Broche, F. H. Labeed, and M. P. Hughes, "Extraction of dielectric properties of multiple populations from dielectrophoretic collection spectrum data," *Phys. Med. Biol.* **50**, 2267 (2005).
- <sup>12</sup>D. J. Bakewell, M. P. Hughes, J. J. Milner, and H. Morgan, "Dielectrophoretic manipulation of avidin and DNA," in *Proceedings of the 20th Annual*

*International Conference of the IEEE Engineering in Medicine and Biology Society* (IEEE, 1998), pp. 1079–1082.

<sup>15</sup>L. Zheng, J. P. Brody, and P. J. Burke, “Electronic manipulation of DNA, proteins, and nanoparticles for potential circuit assembly,” *Biosens. Bioelectron.* **20**, 606–619 (2004).

<sup>16</sup>M. Washizu, S. Suzuki, O. Kurosawa, T. Nishizaka, and T. Shinohara, “Molecular dielectrophoresis of biopolymers,” *IEEE. Trans. Ind. Appl.* **30**, 835–843 (1994).

<sup>17</sup>A. Nakano and A. Ros, “Protein dielectrophoresis: Advances, challenges, and applications,” *Electrophoresis* **34**, 1085–1096 (2013).

<sup>18</sup>K. Keim, M. Z. Rashed, S. C. Kilchenmann, A. Delattre, A. F. Gonçalves, P. Éry, and C. Guiducci, “On-chip technology for single-cell arraying, electrorotation-based analysis and selective release,” *Electrophoresis* **40**, 1830–1838 (2019).

<sup>19</sup>L. Huang, P. Zhao, and W. Wang, “3D cell electrorotation and imaging for measuring multiple cellular biophysical properties,” *Lab Chip* **18**, 2359–2368 (2018).

<sup>20</sup>G. Fuhr, R. Glaser, and R. Hagedorn, “Rotation of dielectrics in a rotating electric high-frequency field. Model experiments and theoretical explanation of the rotation effect of living cells,” *Biophys. J.* **49**, 395–402 (1986).

<sup>21</sup>U. Lei, P.-H. Sun, and R. Pethig, “Refinement of the theory for extracting cell dielectric properties from dielectrophoresis and electrorotation experiments,” *Biomicrofluidics* **5**, 044109 (2011).

<sup>22</sup>S.-B. Huang, Y. Zhao, D. Chen, H.-C. Lee, Y. Luo, T.-K. Chiu, J. Wang, J. Chen, and M.-H. Wu, “A clogging-free microfluidic platform with an incorporated pneumatically driven membrane-based active valve enabling specific membrane capacitance and cytoplasm conductivity characterization of single cells,” *Sens. Actuators B* **190**, 928–936 (2014).

<sup>23</sup>L.-S. Jang and M.-H. Wang, “Microfluidic device for cell capture and impedance measurement,” *Biomed. Microdevices* **9**, 737–743 (2007).

<sup>24</sup>V. Velasco, M. Gruenthal, E. Zusstone, J. M. D. Thomas, R. E. Berson, R. S. Keynton, and S. J. Williams, “An orbital shear platform for real-time, in vitro endothelium characterization,” *Biotechnology and Bioengineering* **113**(6), 1336–1344 (2016).

<sup>25</sup>J. Chen, Y. Zheng, Q. Tan, Y. L. Zhang, J. Li, W. R. Geddie, M. A. Jewett, and Y. Sun, “A microfluidic device for simultaneous electrical and mechanical measurements on single cells,” *Biomicrofluidics* **5**, 014113 (2011).

<sup>26</sup>R. R. Pethig, *Dielectrophoresis: Theory, methodology and biological application in The Clausius-Mossotti Factor* (John Wiley & Sons, Ltd 2017), Chapter 6, pp. 119–144.

<sup>27</sup>S. Williams, “Dielectrophoretic motion of particles and cells,” in *Encyclopedia of Microfluidics and Nanofluidics*, edited by D. Li (Springer, 2008), pp. 357–364.

<sup>28</sup>T. B. Jones, “Basic theory of dielectrophoresis and electrorotation,” *IEEE Eng. Med. Biol. Mag.* **22**, 33–42 (2003).

<sup>29</sup>H. A. Pohl, “Dielectrophoresis: The behavior of neutral matter in nonuniform electric fields” (Cambridge University Press, 1978).

<sup>30</sup>M. González, I. Martín-Ruiz, S. Jiménez, L. Pirone, R. Barrio, and J. D. Sutherland, “Generation of stable *Drosophila* cell lines using multicistronic vectors,” *Sci. Rep.* **1**, 75 (2011).

<sup>31</sup>L. C. Boswell and S. C. Hand, “Intracellular localization of group 3 LEA proteins in embryos of *Artemia franciscana*,” *Tissue Cell* **46**, 514–519 (2014).

<sup>32</sup>F. H. Labeed, H. M. Coley, H. Thomas, and M. P. Hughes, “Assessment of multidrug resistance reversal using dielectrophoresis and flow cytometry,” *Biophys. J.* **85**, 2028–2034 (2003).

<sup>33</sup>S. C. Hand and M. A. Menze, “Molecular approaches for improving desiccation tolerance: Insights from the brine shrimp *Artemia franciscana*,” *Planta* **242**, 379–388 (2015).

<sup>34</sup>A. Ramos, H. Morgan, N. G. Green, and A. Castellanos, “Ac electrokinetics: A review of forces in microelectrode structures,” *J. Phys. D: Appl. Phys.* **31**, 2338 (1998).

<sup>35</sup>W. Liang, Y. Zhao, L. Liu, Y. Wang, W. J. Li, and G.-B. Lee, “Determination of cell membrane capacitance and conductance via optically induced electrokinetics,” *Biophys. J.* **113**, 1531–1539 (2017).

<sup>36</sup>R. Pethig, L. Jakubek, R. Sanger, E. Heart, E. D. Corson, and P. J. Smith, “Electrokinetic measurements of membrane capacitance and conductance for pancreatic  $\beta$ -cells,” in *IEE Proceedings-Nanobiotechnology* (IET, 2005), Vol. 152, pp. 189–193.

<sup>37</sup>E. A. Henslee, P. Crosby, S. J. Kitcatt, J. S. Parry, A. Bernardini, R. G. Abdallat, G. Braun, H. O. Fatoyinbo, E. J. Harrison, R. S. Edgar *et al.*, “Rhythmic potassium transport regulates the Circadian clock in human red blood cells,” *Nat. Commun.* **8**, 1978 (2017).

<sup>38</sup>H. Li, A. Erbas, J. Zwanikken, and M. Olvera de la Cruz, “Ionic conductivity in polyelectrolyte hydrogels,” *Macromolecules* **49**, 9239–9246 (2016).

<sup>39</sup>F. Bordi, R. H. Colby, C. Cametti, L. De Lorenzo, and T. Gili, “Electrical conductivity of polyelectrolyte solutions in the semidilute and concentrated regime: The role of counterion condensation,” *J. Phys. Chem. B* **106**, 6887–6893 (2002).

<sup>40</sup>K. Asami, “Dielectric properties of microvillous cells simulated by the three-dimensional finite-element method,” *Bioelectrochemistry* **81**, 28–33 (2011).

<sup>41</sup>W. R. Loewenstein and Y. Kanno, “Some electrical properties of the membrane of a cell nucleus,” *Nature* **195**, 462 (1962).

<sup>42</sup>A. Irimajiri, K. Asami, T. Ichinowatari, and Y. Kinoshita, “Passive electrical properties of the membrane and cytoplasm of cultured rat basophil leukemia cells. II. Effects of osmotic perturbation,” *Biochim. Biophys. Acta* **896**, 214–223 (1987).

<sup>43</sup>V. L. Sukhorukov, W. M. Arnold, and U. Zimmermann, “Hypotonically induced changes in the plasma membrane of cultured mammalian cells,” *J. Membr. Biol.* **132**, 27–40 (1993).

<sup>44</sup>X.-B. Wang, Y. Huang, P. R. Gascoyne, F. F. Becker, R. Hölzel, and R. Pethig, “Changes in friend murine erythroleukaemia cell membranes during induced differentiation determined by electrorotation,” *Biochim. Biophys. Acta* **1193**, 330–344 (1994).

<sup>45</sup>X.-F. Zhou, G. H. Markx, R. Pethig, and I. M. Eastwood, “Differentiation of viable and non-viable bacterial biofilms using electrorotation,” *Biochim. Biophys. Acta* **1245**, 85–93 (1995).

<sup>46</sup>K. F. Hoettges, J. W. Dale, and M. P. Hughes, “Rapid determination of antibiotic resistance in *E. coli* using dielectrophoresis,” *Phys. Med. Biol.* **52**, 6001 (2007).

<sup>47</sup>H. Pauly, “Electrical conductance and dielectric constant of the interior of erythrocytes,” *Nature* **183**, 333 (1959).

<sup>48</sup>H. Schwan, “Alternating current spectroscopy of biological substances,” *Proc. IRE* **47**, 1841–1855 (1959).

<sup>49</sup>R. Pethig and D. B. Kell, “The passive electrical properties of biological systems: Their significance in physiology, biophysics and biotechnology,” *Phys. Med. Biol.* **32**, 933 (1987).

<sup>50</sup>L. J. Gentet, G. J. Stuart, and J. D. Clements, “Direct measurement of specific membrane capacitance in neurons,” *Biophys. J.* **79**, 314–320 (2000).

<sup>51</sup>M. Stoneman, A. Chaturvedi, D. Jansma, M. Kosempa, C. Zeng, and V. Raicu, “Protein influence on the plasma membrane dielectric properties: In vivo study utilizing dielectric spectroscopy and fluorescence microscopy,” *Bioelectrochemistry* **70**, 542–550 (2007).

<sup>52</sup>M. Muratore, V. Srsen, M. Waterfall, A. Downes, and R. Pethig, “Biomarker-free dielectrophoretic sorting of differentiating myoblast multipotent progenitor cells and their membrane analysis by Raman spectroscopy,” *Biomicrofluidics* **6**, 034113 (2012).